JOURNAL OF AGRICULTURAL AND FOOD CHEMISTRY

ARTICLE

pubs.acs.org/JAFC

Improved Lateral Discrimination in Screening the Elemental Composition of Buckwheat Grain by Micro-PIXE

Paula Pongrac,[†,‡] Katarina Vogel-Mikuš,[‡] Marjana Regvar,[‡] Primož Vavpetič,[†] Primož Pelicon,[†] and Ivan Kreft[*,‡]

[†]Jožef Stefan Institute, Jamova 39, SI-1000 Ljubljana, Slovenia

[‡]Biotechnical Faculty, University of Ljubljana, Jamnikarjeva 101, SI-1000 Ljubljana, Slovenia

ABSTRACT: The elemental composition of specific fractions of cereal and pseudocereal grains can be roughly estimated after milling. Alternatively, the elemental localization of cross-sectioned grains can be quantitatively analyzed by microproton induced X-ray emission (micro-PIXE), taking advantage of high elemental sensitivity and low lateral resolution. We present a micro-PIXE study on buckwheat (*Fagopyrum esculentum*) grain, with a detailed description of the elemental distributions. Elements such as Mg, P, S, K, Fe, Ni, Cu, and Zn were preferentially localized in the cotyledons and embryonic axis; however, significant amounts of K and Fe were also found in the pericarp. The aleurone layer covering the cotyledons was especially enriched in S and P, while testa, a thin layer above the aleurone did not show any significant element enrichments. The highest concentrations of Al, Si, Cl, Ca, and Ti were found in the pericarp. A detailed element localization study of pericarp layers revealed that the inner layer was enriched in K, Mn, Ca, and Fe, while the outer layer showed enrichments in Na, Mg, P, S, and Al. On the basis of the data obtained, milling techniques can be adapted to obtain milling fractions with targeted nutritional values.

KEYWORDS: Buckwheat, *Fagopyrum esculentum*, trace elements, composition, nutritional value, milling fractions

INTRODUCTION

Consumption of the grains of common buckwheat (*Fagopyrum esculentum* Moench; Polygonaceae), as part of an everyday diet, has increased over the past few years. It is well established that buckwheat is a rich source of high quality protein, with a balanced amino-acid composition,[1] dietary fiber,[2] and retrograded starch,[3] and high quality lipids, vitamins, essential minerals,[1,4,5] and antioxidants, such as rutin.[6] Additionally, it is gluten-free, and thus it provides an important alternative nutritious food for people with celiac disease.[7]

The mature grain of common buckwheat is a triangular achene that consists of the pericarp (hull), spermoderm (testa), aleurone layer, endosperm, and embryo. The pericarp is made up of the epicarp, a thick-walled fiber layer, the elongated parenchyma cells of the pigment layer, and the large longitudinally elongated cells of the endocarp.[8,9] The testa consists of the outer epiderm of longitudinally elongated wavy cells, the spongy parenchyma, and the inner epiderm, which is closely attached to the aleurone layer.[9] The nonstarchy aleurone layer consists of a single row of cells, and it is 10−15 μm thick.[10] In the endosperm, there are large, thin-walled, closely packed cells that are filled with starch.[11] The embryo consists of the embryonic axis and two cotyledons, with a thickness of 130−170 μm; the cells are separated by their 1-μm-thick cell walls.[12]

For consumption, buckwheat grains are milled to produce different fractions, which typically comprise the groats (dehulled seed), different types of flour (mainly, but not solely, consisting of endosperm particles), and bran (testa and some embryo tissues).[13,14] These fractions differ in their elemental compositions and elemental concentrations, which can significantly influence the nutritional quality of the products. For instance, lower concentrations of trace elements have been found in flour than in the pericarp[15] and in the bran.[2,4] Additionally, during traditional preparation of buckwheat groats, there is a significant migration of the substances between the pericarp and the groats.[16] By determining the concentrations of the elements in chemically or mechanically disturbed tissues (the milling fractions) and those mixed in terms of their origin, it is difficult to establish the importance of different tissues for the composition of individual milling fractions and products. Thus, it is very important to establish the concentrations and localizations of elements in the intact grain. One appropriate analytical technique is microproton induced X-ray emission (micro-PIXE), which does not require chemical destruction or milling of the grain to reveal the elemental composition of particular tissues or layers. In our preliminary study using micro-PIXE, we have demonstrated that in common buckwheat grain, Mg, P, S, Mn, K, Cu, Zn, and Fe mostly accumulate in the cotyledons, while the endosperm is a modest trace-element source.[17] In the present study, we report on the data from our extended micro-PIXE study of common buckwheat grain, in which further aspects have now been included, as compared to our previous report: (i) improved cross-section of the grain, in which the whole embryo is seen (both the embryonic axis and cotyledons); (ii) improved spectral statistics, through prolonged measurement times; and (iii) optimized positioning of the samples to achieve optimal contrast on the pericarp layers. The aim of the present study was to determine the elemental distributions among the parts of the common buckwheat grain, and to assess in detail the elemental composition of the different

Received: August 13, 2010
Accepted: December 21, 2010
Revised: December 15, 2010
Published: January 12, 2011

dx.doi.org/10.1021/jf103150d | *J. Agric. Food Chem.* 2011, 59, 1275–1280

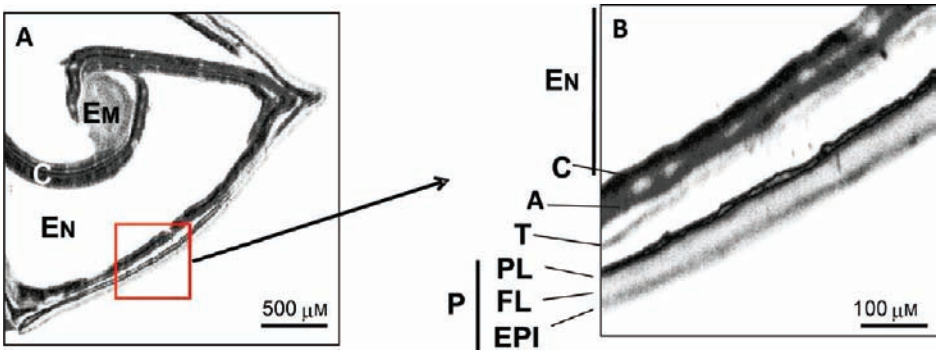

Figure 1. Cross-section of common buckwheat grain as analyzed by micro-PIXE. (A) Grain cross-section and (B) higher magnification of boxed area in A, obtained by gray scaling the potassium distribution map (see Figures 2 and 3). A, aleurone; C, cotyledons; En, endosperm; Em, embryonic axis; EPI, epicarp; FL, fiber layer; P, pericarp; PL, pigment layer; and T, testa.

layers, with specific reference to the perikarp, and thus add to the existing current knowledge on buckwheat grain composition.

MATERIALS AND METHODS

Common buckwheat (*Fagopyrum esculentum* Moench), cv. Darja was grown in the experimental fields of the Biotechnical Faculty of the University of Ljubljana, Ljubljana, Slovenia (320 m above sea level; 46°35′N, 14°55′E). The mature grain was collected in October 2007. The dried grains (containing on average 10% of water) were cut into 2-mm-thick sections with a stainless steel scalpel, and the sections were then individually mounted between two thin layers of Pioloform foil stretched over an aluminum frame.[17,18]

The images of the cross-sections were obtained with an Axioscop 2 MOT microscope (Carl Zeiss, Goettingen, Germany), using a visible, blue-light and UV-light excitation source, equipped with an Axiocam MRc color digital camera, using AxioVision 4.1 software.

The micro-PIXE analysis was performed with the nuclear microprobe in the tandetron accelerator laboratory of Jožef Stefan Institute (Ljubljana, Slovenia).[19,20] The grain sections were raster scanned using a proton microbeam (2 × 2 μm; ion current, approximately 400 pA). The selected beam energy was 2 MeV, with a maximum scanning area of 2,500 × 2,500 μm^2. The samples were mounted onto a five-axis motorized vacuum goniometer with a positioning precision of 1 μm. The positioning of the sample in the focal plane of the quadruple triplet lens with a precision better than 60 μm was obtained by bringing the sample surface into the depth of field of the optical microscope.

Detection of X-ray energies from 1 to 25 keV was achieved using two X-ray detectors: a high-purity germanium X-ray detector (active area, 95 mm^2; beryllium window, 25 μm thick; polyimide absorber, 100 μm thick) positioned at 135° with respect to the beam direction; and a Si(Li) detector (active area, 10 mm^2) positioned at 125° with respect to the beam direction; this latter was for the detection of low energy X-rays of 0.8−4.0 keV.

For precise proton dose determination, an in-beam chopping device (gold-plated graphite; beam intersection frequency, approximately 10 Hz) was positioned in the beamline after the last collimation of the beam, before it hit the sample. This thus made the system insensitive to beam intensity fluctuations and any electrical conductivity of the sample. The spectrum of backscattered protons from the chopper was recorded in parallel with the PIXE spectra in list mode. This high-energy part of the spectrum consisted of protons scattered from the Au layer and appeared as a separate peak. During off-line data processing, the spectrum accumulated at the in-beam chopper over an arbitrary scanning area could be extracted from the list-mode data simultaneously with the PIXE spectra and used for dose information.[17]

The morphological structures of the common buckwheat grain are shown in Figure 1. The X-ray spectra emitted from the distinct grain structures were extracted from the list-mode files over the regions selected. The spectra were analyzed using the GupixWin package.[21] The setup used thick sample description and trace element calculations based on a starch matrix. The edges of the target oriented toward the corresponding X-ray detector were avoided in the evaluation, as the description of the X-ray absorption at the X-ray exit path was not correctly evaluated in this particular case.

Four buckwheat grains were scanned using micro-PIXE, and the average concentrations of the detected elements are given in Table 1. The efficiencies of the Ge and Si(Li) X-ray detectors were determined by measuring a large series of monoelemental targets and certified standards. In the first step, the technical characteristics of the detectors were loaded into the GupixWin program, with the results described optimally by an optimized dead-layer thickness. These efficiency descriptions still lacked a precision better than 15% in the energy regions close to the Ge and Si absorption edges of the respective detectors. Additional efficiency dependences were loaded into the GupixWin program to account for these discrepancies and to obtain data with the monoelemental samples significantly better than 10% error. In the final calibration step, the method was tested on Standard Reference Materials National Institutes for Standards and Technology (NIST) Naval Brass (C1107) and NIST Tomato Leaves (1573a). The precision was verified in intercomparative studies using X-ray fluorescence, atomic emission spectrometry, inductively coupled plasma mass spectrometry, and micro-PIXE, on homogenized, dry, bulk plant material.[22]

Colocalization analysis of intensities between particular elements was performed on 8-bit elemental maps by the ImageJ (http://rsb.info.nih.gov/ij/) program using plug-in Intensity correlation analysis, generating Pearson's correlation coefficients (r) (http://www.macbiophotonics.ca/imagej/colour_analysis.htm). Pearson's correlation coefficients range from 1 to −1, where a value of 1 represents perfect correlation/colocalization; a value of −1 represents perfect exclusion; and zero represents random localization.

Statistical analysis of element concentrations was performed using Statistica Statsoft 7.0 software. Duncan's test was used to calculate the differences in concentrations between particular tissues in buckwheat grain.

RESULTS AND DISCUSSION

To determine the localization of the elements, cross-sections of the whole common buckwheat grain and a further smaller area encompassing the endosperm, cotyledons, aleurone, testa, and pericarp were scanned using micro-PIXE (Figure 1). The elemental maps obtained revealed the spatial distributions of Na, Mg, Al, Si, P, S, Cl, K, Ca, Mn, and Zn in the whole-grain cross-section (Figure 2), while for Fe the number of counts was too low to be able to obtain a map with satisfactory statistics.

Table 1. Average Concentrations ($\mu g\ g^{-1}$) of Elements in Specific Indicated Tissues of Four Grains of Common Buckwheat As Obtained by Micro-PIXE[a]

Micro-PIXE: Scanned area 2,500 x 2,500 μm² (highlighted)															
	Whole area			Endosperm			Embryo Cotyledons			Embryo Embryonic axis			Pericarp		
El.	Conc.	se	LOD	Conc.	se	LOD	Conc.	se	LOD	Conc.	se	LOD	Conc.	se	LOD
Mg	1760	439	65.6	135 a	45.7	80.6	7260 b	1990	218	2750 ab	875	303	3650 ab	1650	428
Al	62.2	23.2	35.5	24.3 a	3.11	38.8	204 b	72.8	137	441 b	88.3	173	373 b	111	203
Si	>LOD	>LOD	53.9	110 a	32.6	28.0	>LOD a	>LOD	198	>LOD a	>LOD	247	513 b	149	129
P	3790	1060	26.2	139 a	31.9	29.2	16500 b	4630	107	7630 b	2440	123	733 a	207	127
S	1130	254	16.2	323 a	81.2	20.6	3610 b	782	53.0	2680 b	611	67.3	483 a	186	89.8
Cl	159	40.8	12.7	73.4 a	32.3	16.3	246 a	61.3	42.6	50.0 a	5.00	59.9	782 b	327	71.3
K	4470	941	11.6	264 a	74.4	12.7	16400 b	4030	39.2	6820 ab	1860	55.2	6780 ab	2270	51.5
Ca	261	27.9	21.6	70.4 a	17.1	11.3	221 a	38.6	93.6	214 a	51.9	86.0	1590 b	405	84.9
Ti	8.98	0.99	1.25	11.8 a	5.55	3.08	9.8 a	4.42	3.95	2.60 a	0.50	7.08	95.7 a	15.9	4.71
Mn	8.55	1.98	0.65	>LOD a	>LOD	1.21	26.8 a	4.24	2.37	29.0 a	18.3	3.33	33.7 a	11.2	1.55
Fe	23.4	0.68	0.71	10.0 a	1.69	0.59	76.2 c	12.2	3.23	39.2 ab	6.43	4.43	56.0 bc	5.06	3.80
Ni	0.51	0.08	0.40	>LOD a	>LOD	0.70	2.23 b	0.72	1.38	1.50 ab	0.50	3.99	>LOD a	>LOD	1.95
Cu	3.98	0.68	0.42	1.30 a	0.18	0.50	7.48 b	1.28	1.65	5.90 b	0.49	1.84	2.40 a	0.49	1.90
Zn	14.3	2.66	0.29	1.52 a	0.39	0.45	63.3 b	15.1	1.68	52.3 b	5.09	5.85	3.70 a	1.06	2.20

[a] Conc., concentration ($\mu g\ g^{-1}$); se, standard error ($\mu g\ g^{-1}$); El., element; LOD, limit of detection ($\mu g\ g^{-1}$). Different letters beside the average values represent statistically significant differences among element concentrations in particular tissues. Duncan's test, $p < 0.05$.

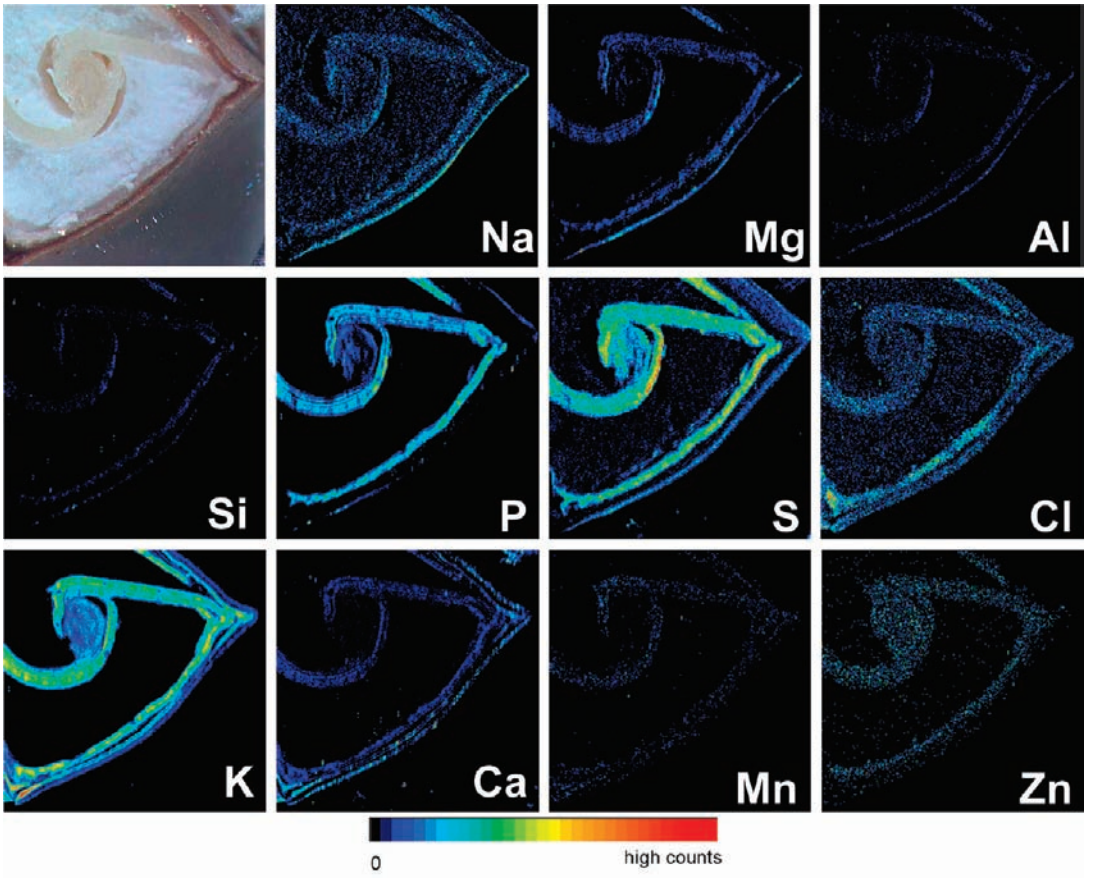

Figure 2. Cross-section of common buckwheat grain as analyzed by light microscopy and micro-PIXE. Light microscopy (top left panel only) and qualitative elemental maps of Na, Mg, Al, Si, P, S, Cl, K, Ca, Mn, and Zn (as indicated). Scan size: 2,500 × 2,500 μm^2.

The endosperm was poor in trace elements, with the lowest concentrations of all the elements detected (Table 1), as has already been shown.[17] This is the reason why buckwheat flour contains lower concentrations of elements in comparison to that

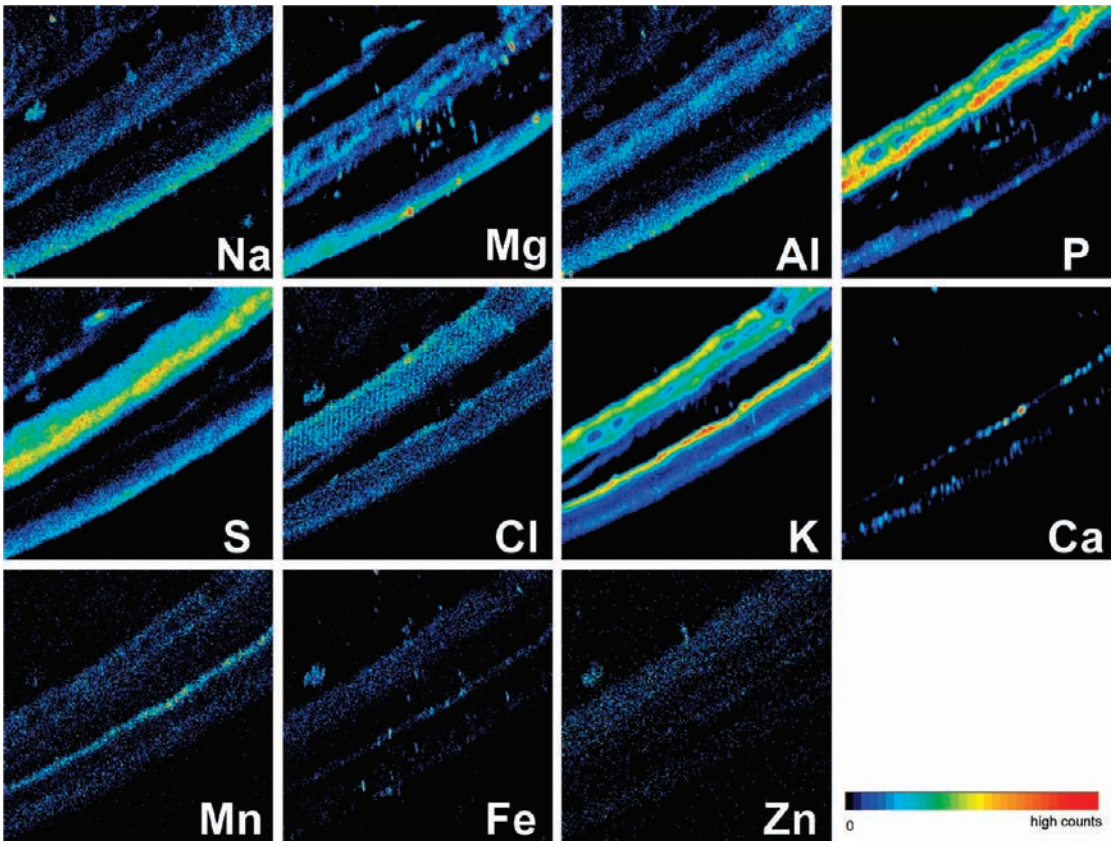

Figure 3. Details of the cross-section of common buckwheat grain as analyzed by micro-PIXE. Qualitative elemental maps of Na, Mg, Al, P, S, Cl, K, Ca, Mn, Fe, and Zn (as indicated) in the pericarp area. Scan size: 500 × 500 μm^2.

in bran, in different milling conditions.[1,2] However, buckwheat flour was shown to have higher concentrations of Cu, Mn, Mg, K, and P, as compared to wheat, rice, and maize flours, with the highest proportions of Zn released as a soluble form after enzymatic digestion in vitro.[23]

The majority of the elements detected were localized in the cotyledons, although not all of these elements were found in the same concentrations in the embryonic axis (Figure 2). Phosphorus showed high level of colocalization with Zn (r = 0.70), Cl (r = 0.69), Na (r = 0.68), and Mn (0.63) confirming the association of especially Zn and Mn with the phytate part of the total phosphorus. Binding of Mn and Zn to the same anionic component was additionally supported by a high level of their colocalization (r = 0.86). Potassium showed significant colocalization with P (r = 0.83), S (r = 0.82), and Cl (r = 0.70) indicating its binding to the P, S, and Cl anions present in embryonic tissues. Mg distribution was strongly correlated to that of Al (r = 0.93), Mn (r = 0.91), Na (r = 0.86), Zn (r = 0.83), Si (r = 0.80), and Ca (r = 0.86), mainly because of the high abundance of the mentioned elements in embryonic tissues and the pericarp. Except Fe, the concentrations of the elements detected in the embryo were not significantly different from that in the cotyledons (Table 1). In the literature, information on the elemental compositions and concentrations in the buckwheat embryo is scarce; as in the bran-milling fraction, these grain parts are usually included along with some particles of the testa and pericarp.[2] The bran fraction is known to be the fraction that is of the most value in terms of nutritional components, as it is concentrated in protein, lipid, dietary fiber, and fagopyritols.[2] Less mobile elements such as Ca, Si, Al, and Ti were present in the highest concentrations in the pericarp, although the pericarp also contained high concentrations of Mg, K, and Cl (Table 1).

In order to better distinguish the elemental distributions in particular layers, a zoomed area of the outer border of the cross-section was scanned (Figure 1B), and their elemental distribution maps are given in Figure 3. As well as the elementally poor endosperm (Figure 3, upper left corner), the elementally rich cotyledon, and the layers of the pericarp, a layer between the cotyledons and the pericarp, the aleurone, can be seen as an enrichment of P, S, and some Mg covering the lower part of cotyledon. Since the aleurone in buckwheat plays similar role during germination as, for example, in monocotyledonous wheat, P and S enrichment probably correlates with high concentrations of phytate and proteins in this layer. The aleurone cells are small and are only 10−15 μm in width,[10] which corresponds to the thickness of the mentioned layer in Figures 1 and 3, and the testa is multilayered but very thin[8] covering the aleurone layer and showing no particular enrichments of elements detected in a seed. In the pericarp, the spatial distributions of Na, Mg, Al, P, S, Cl, K, Ca, Mn, Fe, and Zn illustrated the differential elemental compositions of this particular layer (Figure 3). Two layers of the pericarp with different compositions can be easily distinguished, the inner and outer layer, particularly on the basis of the K, Ca, Mn, and Fe distribution maps, with the inner layer showing enrichments in K, Mn, Fe, and Ca and the outer layer showing enrichments in Na, Mg, Al, P, and S. As the layers of the pericarp are tightly bound to each other, they cannot be precisely mechanically separated, and it has not been previously possible to

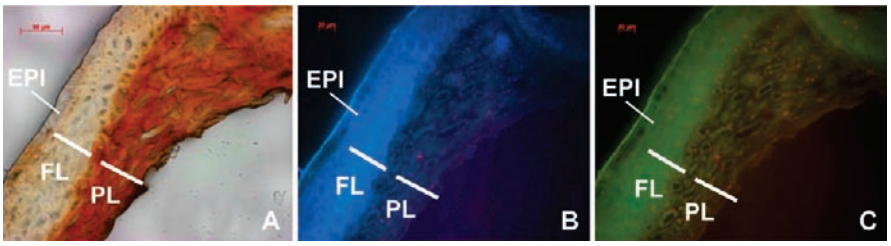

Figure 4. Details of the cross-section of common buckwheat grain as analyzed by light microscopy. (A) Visible light, (B) UV light, and (C) blue light source excitation. EPI, epicarp; FL, fiber layer; and PL, pigment layer.

determine these differences in their elemental compositions. Morphological structures of the pericarp layers at the micrometer scale have been studied by electron microscope.[9] To make the elemental distribution of pericarp layers easier to distinguish, thin sections of the pericarp were photographed under optical microscope using blue-light and UV-light excitation to enhance the visualization of these layers (Figure 4). The epicarp is a one-cell layer by a thick-walled fiber layer and a brown pigmented layer that were all easily distinguished using visual light (Figure 4A). Under blue and UV excitation blue (546 nm) and UV (470 nm), the fiber layer showed the highest autofluorescence (Figures 4B,C). Blue autofluorescence upon UV excitation is an indication of a high content of polyphenolics, such as lignin,[24] aromatic suberin polymers,[25] or other aromatic compounds in the cell walls. Yellow to green autofluorescence upon blue excitation can, however, indicate that the cell walls contain flavins.[26] In onion cells, blue-light-induced green autofluorescence of flavonols has been described.[27] Bulk studies of pericarp have shown that it has the highest concentrations of flavonoids and especially rutin,[2] which might be the substance emitting the green autofluorescence upon blue excitation. With the help of the microscopic photographs, we can conclude that the two layers seen in the elemental maps correspond to the pigmented layer (the inner layer) and to the fiber layer and pericarp (the outer layer).

As most of the pericarp is removed from buckwheat grain during its processing, it is usually not included in bulk analyses. However, it has been seen that during traditional processing, i.e., hydro-thermal treatment before the removal of the pericarp, some substances can be transferred from the pericarp to the seed, and vice versa.[16] Besides the straw and leaves, the pericarp is the major byproduct of buckwheat flour production.[15] In some cases, the pericarp is included in the fractions intended for human consumption, especially as it is rich in rutin,[2] and thus, its elemental composition can have a role in health-related use of buckwheat milling products.

The micro-PIXE technique has been successfully applied to different plant parts, such as seeds,[17,28] leaves,[29−31] stalks,[32] and roots,[18,33] although with limited lateral discrimination. The advantages of the present, improved method for our buckwheat grain investigation can be seen in the high elemental sensitivity, the quantification of the data, the micrometer lateral resolution, and the possibility to overcome problems that arise from determining the concentrations of elements in chemically or mechanically (milling fraction) disturbed tissues, which can lead to element redistribution or losses.[34] Additionally, our analytical setup enables off-line analysis, in which the specific tissue is defined, and the spectra of only that area can be used to calculate the concentrations of the elements. These reasons make micro-PIXE a state-of-the-art technique among localization studies in edible grain. Furthermore, this in-depth micro-PIXE study of common buckwheat grain is based on advances relating to the suitable cross-sectioning of the grain, the increased times for measurements, and the optimized positioning of the samples in relation to the beam to achieve optimal contrast for the pericarp layers. The lessons learned here can now be applied to the grains of additional different cereals and pseudocereals that can be prepared for such micro-PIXE analyses by simply being cut sharply in half.

AUTHOR INFORMATION

Corresponding Author

*Tel: +3861 320 3261. Fax: +3861 423 1088. E-mail: ivan.kreft@guest.arnes.si.

Funding Sources

The study was financed by the following programs and projects of Slovenian Research Agency: P1-0212, P1-0112, J7-0352, J4-3618, Fellowships for "Young Researchers", Support of the Accelerator Laboratory in the framework of Research Infrastructure. Part of the study was carried out within EU Project COST 859 and EU FP7 Project No. 2270112 "SPIRIT". A scholarship from the World Federation of Scientists and a National Fellowship awarded by L'OREAL-UNESCO-The Slovenian Science Foundation to P.P. are gratefully acknowledged.

ABBREVIATIONS USED

micro-PIXE, microproton induced X-ray emission; NIST, National Institute for Standards and Technology.

REFERENCES

(1) Bonafaccia, G.; Marocchini, M.; Kreft, I. Composition and technological properties of the flour and bran from common and tartary buckwheat. *Food Chem.* **2003**, *80*, 9–15.

(2) Steadman, K. J.; Burgoon, M. S.; Lewis, B. A.; Edwardson, S. E.; Obendorf, R. L. Minerals, phytic acid, tannin and rutin in buckwheat seed milling fractions. *J. Sci. Food Agric.* **2001**, *81*, 1094–1100.

(3) Kreft, I.; Skrabanja, V. Nutritional properties of starch in buckwheat noodles. *J. Nutr. Sci. Vitaminol.* **2002**, *48*, 47–50.

(4) Bonafaccia, G.; Gambelli, L.; Fabjan, N.; Kreft, I. Trace elements in flour and bran from common and tartary buckwheat. *Food Chem.* **2003**, *83*, 1–5.

(5) Skrabanja, V.; Elmstahl, H.; Kreft, I.; Bjorck, I. M. E. Nutritional properties of starch in buckwheat products: Studies *in vitro* and *in vivo*. *J. Agric. Food Chem.* **2001**, *49*, 490–496.

(6) Kreft, I.; Fabjan, N.; Yasumoto, K. Rutin content in buckwheat (*Fagopyrum esculentum* Moench) food materials and products. *Food Chem.* **2006**, *98*, 508–512.

(7) Alvarez-Jubete, L.; Arendt, E. K.; Gallagher, E. Nutritive value and chemical composition of pseudocereals as gluten-free ingredients. *Int. J. Food Sci. Nutr.* **2009**, *60*, 240–257.

(8) Pomeranz, Y.; Sachs, I. B. Scanning electron microscopy of buckwheat kernel. *Cereal Chem.* **1972**, *49*, 23–25.

(9) Pomeranz, Y. Buckwheat: structure, composition, and utilization. *Crit. Rev. Food Sci. Nutr.* **1983**, *19*, 213–258.
(10) Javornik, B.; Kreft, I. Structure of Buckwheat Kernel. In *Buckwheat*; IBRA: Ljubljana, Yugoslavia, 1980; pp 105−114.
(11) Stevens, N. E. The morphology of the seed of buckwheat. *Bot. Gaz.* **1912**, *53*, 59–66.
(12) Škrabanja, V.; Kreft, I.; Golob, T.; Modic, M.; Ikeda, S.; Ikeda, K.; Kreft, S.; Bonafaccia, G.; Knapp, M.; Kosmelj, K. Nutrient content in buckwheat milling fractions. *Cereal Chem.* **2004**, *81*, 172–176.
(13) Fornal, J.; Soral-Smietana, M.; Fornal, L. Buckwheat groats production. 2. The changes in the ultrastructure of buckwheat (*Fagopyrum esculentum* Moench) during processing. *Nahrung-Food* **1981**, *25*, 353–358.
(14) Kreft, I. *Ajda.* ČZD Kmečki glas: Slovenia, 1995; p 112.
(15) Ikeda, S.; Yamashita, Y.; Kreft, I. Mineral composition of buckwheat by-products and its processing characteristics to konjak preparation. *Fagopyrum* **1999**, *16*, 89–94.
(16) Janeš, D.; Prosen, H.; Kreft, I.; Kreft, S. Aroma compounds in buckwheat (*Fagopyrum esculentum* Moench) groats, flour, bran, and husk. *Cereal Chem.* **2010**, *87*, 141–143.
(17) Vogel-Mikuš, K.; Pelicon, P.; Vavpetic, P.; Kreft, I.; Regvar, M. Elemental analysis of edible grains by micro-PIXE: Common buckwheat case study. *Nucl. Instrum. Methods Phys. Res., Sect. B* **2009**, *267*, 2884–2889.
(18) Vogel-Mikuš, K.; Pongrac, P.; Pelicon, P.; Vavpetič, P.; Povh, B.; Bothe, H.; Regvar, M. Micro-PIXE Analysis for Localisation and Quantification of Elements in Roots of Mycorrhizal Metal-Tolerant Plants. In *Symbiotic Fungi: Principles and Practice*; Varma, A., Kharkwal, A., Eds.; Springer-Verlag: New York, 2009; Vol. 18, pp 227−242.
(19) Simčič, J.; Pelicon, P.; Budnar, M.; Šmit, Ž. The performance of the Ljubljana ion microprobe. *Nucl. Instrum. Methods Phys. Res., Sect. B* **2002**, *190*, 283–286.
(20) Pelicon, P.; Simčič, J.; Jakšič, M.; Medunić, Z.; Naab, F.; Mcdaniel, F. D. Spherical chamber-effective solution for multipurpose nuclear microprobe. *Nucl. Instrum. Methods Phys. Res., Sect. B* **2005**, *231*, 53–59.
(21) Campbell, J. L.; Hopman, T. L.; Maxwell, J. A.; Nejedly, Z. The Guelph PIXE software package III: Alternative proton database. *Nucl. Instrum. Methods Phys. Res., Sect. B* **2000**, *170*, 193–204.
(22) Nečemer, M.; Kump, P.; Ščančar, J.; Jačimović, R.; Simčič, J.; Pelicon, P.; Budnar, M.; Jeran, Z.; Pongrac, P.; Regvar, M.; Vogel-Mikuš, K. Application of X-ray fluorescence analytical techniques in phytoremediation and plant biology studies. *Spectrochim. Acta, Part B* **2008**, *63*, 1240–1247.
(23) Ikeda, S.; Yamashita, Y.; Tomura, K.; Kreft, I. Nutritional comparison in mineral characteristics between buckwheat and cereals. *Fagopyrum* **2006**, *23*, 61–65.
(24) Willemse, M. T. M. Microsporogenesis *in vivo* and *in vitro* - autofluorescence of pollen wall of *Lilium* and changes in pollen wall of Gasteria in *Lilium* anther. *Acta Soc. Bot. Pol.* **1981**, *50*, 103–110.
(25) Bernards, M. A.; Lewis, N. G. The macromolecular aromatic domain in suberized tissue: A changing paradigm. *Phytochemistry* **1998**, *47*, 915–933.
(26) Billinton, N.; Knight, A. W. Seeing the wood through the trees: A review of techniques for distinguishing green fluorescent protein from endogenous autofluorescence. *Anal. Biochem.* **2001**, *291*, 175–197.
(27) Sudo, E.; Teranishi, M.; Hidema, J.; Taniuchi, T. Visualization of flavonol distribution in the abaxial epidermis of onion scales via detection of its autofluorescence in the absence of chemical processes. *Biosci., Biotechnol., Biochem.* **2009**, *73*, 2107–2109.
(28) Vogel-Mikuš, K.; Pongrac, P.; Kump, P.; Nečemer, M.; Simčič, J.; Pelicon, P.; Budnar, M.; Povh, B.; Regvar, M. Localisation and quantification of elements within seeds of Cd/Zn hyperaccumulator *Thlaspi praecox* by micro-PIXE. *Environ. Pollut.* **2007**, *147*, 50–59.
(29) Vogel-Mikuš, K.; Simčič, J.; Pelicon, P.; Budnar, M.; Kump, P.; Nečemer, M.; Mesjasz-Przybylowicz, J.; Przybylowicz, W. J.; Regvar, M. Comparison of essential and non-essential element distribution in leaves of the Cd/Zn hyperaccumulator *Thlaspi praecox* as revealed by micro-PIXE. *Plant Cell Environ.* **2008**, *31*, 1484–1496.
(30) Vogel-Mikuš, K.; Regvar, M.; Mesjasz-Przybylowicz, J.; Przybylowicz, W. J.; Simčič, J.; Pelicon, P.; Budnar, M. Spatial distribution of cadmium in leaves of metal hyperaccumulating *Thlaspi praecox* using micro-PIXE. *New Phytol.* **2008**, *179*, 712–721.
(31) Pongrac, P.; Vogel-Mikuš, K.; Vavpetič, P.; Tratnik, J.; Regvar, M.; Simčič, J.; Grlj, N.; Pelicon, P. Cd-induced redistribution of elements within leaves of the Cd/Zn hyperaccumulator *Thlaspi praecox* as revealed by micro-PIXE. *Nucl. Instrum. Methods Phys. Res., Sect. B* **2010**, *268*, 2205–2210.
(32) Kachenko, A. G.; Singh, B.; Bhatia, N. P.; Siegele, R. Quantitative elemental localisation in leaves and stems of nickel hyperaccumulating shrub *Hybanthus floribundus* subsp *floribundus* using micro-PIXE spectroscopy. *Nucl. Instrum. Methods Phys. Res., Sect. B* **2008**, *266*, 667–676.
(33) Weiersbye, I. M.; Straker, C. J.; Przybylowicz, W. J. Micro-PIXE mapping of elemental distribution in arbuscular mycorrhizal roots of the grass, *Cynodon dactylon*, from gold and uranium mine tailings. *Nucl. Instrum. Methods Phys. Res., Sect. B* **1999**, *158*, 335–343.
(34) Schneider, T.; Sheloske, S.; Povh, B. A method for cryosectioning of plant roots for proton microprobe analysis. *I. J. PIXE* **2002**, *12*, 101–107.